Cleavage of the Nb=O Bond of Oxoniobium(V) Porphyrins. Synthesis and Characterization of Novel Niobium(V) Porphyrins with Two Distinct Catechols

Masato Kurihara, Noriyuki Katoh, Takahiko Kojima, Yoichi Ishii,† and Yoshihisa Matsuda*

Department of Chemistry, Faculty of Science, Kyushu University, Hakozaki, Higashi-ku, Fukuoka 812, Japan, and Department of Chemistry and Biotechnology, Faculty of Engineering, The University of Tokyo, Hongo, Bunkyo-ku, Tokyo 113, Japan

Received October 20, 1994[⊗]

A novel catecholato complex, Nb^{V}(tpp)(cat)(Hcat), where cat and Hcat are two distinct catechol ligands (a bidentate catecholate dianion and a monodentate catecholate monoanion, respectively) and tpp is 5,10,15,20-tetraphenylporphyrin dianion, has been isolated in the reaction of Nb^{V}(tpp)(O)(AcO) with catechol, where AcO is an acetato ligand. Its molecular structure has been determined by X-ray crystallography. Crystal data: monoclinic, space group $P2_1/c$, $Z = 4$, $a = 14.592(3)$ Å, $b = 23.46(1)$ Å, $c = 14.415(4)$ Å, $\beta = 100.95(2)°$, $R = 0.079$. The molecular structure was confirmed to have no oxo ligand, and in this respect it is unique among the niobium(V) porphyrins. The bidentate and monodentate ligands are located on the same side of the porphyrin ring. The heptacoordinate niobium atom is bonded to the four pyrrole nitrogen atoms and to three oxygen atoms in the catechols. The niobium atom is displaced by 1.02 Å from the mean plane of the four nitrogen atoms. The structure of the complex in solution and the mechanism of the Nb=O cleavage were investigated by means of ^{1}H-NMR spectroscopy. The bidentate catechol is oriented in C_s symmetry with respect to the porphyrin plane, and the monodentate catechol is located perpendicularly to both the bidentate catechol and the porphyrin plane. Two intermediates with the bidentate catechol were observed after addition of 2 equiv of catechol to Nb(tmp)(O)(AcO) at −30 °C, where tmp denotes the 5,10,15,20-tetramesitylporphyrin dianion. These intermediates were determined to be Nb(tmp)(cat)(OH) and Nb(tmp)(cat)(AcO). Thus, the Nb=O bond of Nb(tmp)(O)(AcO) was easily cleaved to create the two intermediates. We propose a unique route to the Nb=O cleavage that involves an intramolecular electron transfer from the catechol ligand coordinated at the first stage through a ligand exchange with AcO. Both protonation and electron transfer to the Nb=O moiety play important roles in the Nb=O cleavage.

Introduction

The early transition metal porphyrins generally possess strongly bound oxygen atoms as axial ligands to form oxo or μ-oxo compounds. The syntheses and characterization of oxometalloporphyrins of niobium(V) were first reported by Buchler and co-workers.[1] Molecular structures of three oxo niobium porphyrins, *i.e.*, an oxo acetato complex (Nb(tpp)(O)(AcO)),[2-4] a tris(μ-oxo) dimer ($\{Nb(tpp)\}_2O_3$),[4-7] and an oxo fluoro complex (Nb(oep)(O)(F))[8] were confirmed by X-ray diffraction measurements. The axial ligands in these complexes are located on the same side with respect to the equatorial porphyrin ligand. The Nb=O bond is highly stable and has not been cleaved by chemical,[9] photochemical,[10] or electrochemical[11] reductions. Therefore, many attempts have been made to synthesize complexes that have no oxo ligands. These complexes were presumed to be good precursors for complexes in oxidation states other than five, because the former might be readily reduced. For this purpose, trihalo complexes, Nb(por)$(X)_3$, have been prepared. A trifluoro complex, Nb(oep)$(F)_3$, was first reported by Buchler and Robock by treatment of $\{Nb(oep)\}_2O_3$ with HF in toluene.[1] Later, trichloro- and tribromoniobium complexes of several porphyrins were prepared by treatment with anhydrous hydrogen halides,[12] but the molecular structures of these complexes have not been clarified by X-ray crystallography. In the formation of the trihalo complexes, the cleavage of the stable Nb=O bond is caused by the protonation of Nb=O by anhydrous hydrogen halides; however, the trihalo complexes are subject to hydrolysis by trace amounts of H_2O, which results in the regeneration of the Nb=O bond.

Exchange reactions of niobium porphyrins with other axial ligands have not been described. Our attempts to isolate a niobium monomer with an alkoxo or phenoxo ligand were unsuccessful due to the fast hydrolysis of the complexes to form the same product, the tris(μ-oxo) dimer. These alkolato or phenolato complexes were the only dominant species in the presence of excess alcohol or phenol.[10] In the case where catechol derivatives were used in place of alcohols or phenols as potential axial ligands, we succeeded in the isolation of

* To whom correspondence should be addressed at Kyushu University.
† The University of Tokyo.
⊗ Abstract published in *Advance ACS Abstracts*, August 1, 1995.

(1) (a) Buchler, J. W.; Rohbock, K. *Inorg. Nucl. Chem., Lett.* **1972**, 8, 1073. (b) Rohbock, K. Dissertation, Technische Hochshule Aachen, 1972. (c) Buchler, J. W.; Puppe, L.; Rohbock, K.; Schneehage, H. H. *Proc. N.Y. Acad. Sci.* **1973**, *116*, 206.
(2) Abbreviations used: tpp, tmp, and oep, for tetraphenyl-, tetramesityl-, and octaethylporphyrin dianion, respectively; AcO, acetato ligand; cat, bidentate catecholate dianion; dbc, bidentate 3,5-di-*tert*-butylcatecholate dianion; Hcat, monodentate catecholate monoanion; Hdbc, monodentate 3,5-di-*tert*-butylcatecholate monoanion.
(3) Lecomte, C.; Protas, J.; Guilard, R.; Fliniaux, B.; Fournari, P. *J. Chem. Soc., Chem. Commun.* **1976**, 434.
(4) Lecomte, C.; Protas, J.; Guilard, R.; Fliniaux, B.; Fournari, P. *J. Chem. Soc., Dalton Trans.* **1979**, 1306.
(5) Johnson, J. F.; Scheidt, W. R. *Inorg. Chem.* **1978**, *17*, 1280.
(6) Lecomte, C.; Protas, J.; Guilard, R. *C. R. Acad. Sci., Ser. C* **1976**, *283*, 397.
(7) Johnson, J. F.; Scheidt, W. R. *J. Am. Chem. Soc.* **1977**, *99*, 294.
(8) Lecomte, C.; Protas, J.; Richard, P.; Barbe, J. M.; Guilard, R. *J. Chem. Soc., Dalton Trans.* **1982**, 247.
(9) Guilard, R.; Richard, P.; el Borai, M.; Laviron, E. *J. Chem. Soc., Chem. Commun.* **1980**, 516.
(10) Matsuda, Y.; Sakamoto, S.; Takaki, T.; Murakami, Y. *Chem. Lett.* **1985**, 107.
(11) Matsuda, Y.; Yamada, S.; Goto, T.; Murakami, Y. *Bull. Chem. Soc. Jpn.* **1981**, *54*, 452.
(12) (a) Green, M. L. H.; Moreau, J. J. E. *Inorg. Chim. Acta* **1978**, *31*, L461. (b) Richard, P.; Guilard, R. *J. Chem. Soc., Chem. Commun.* **1983**, 1454. (c) Richard, P.; Guilard, R. *Nouv. J. Chim.* **1985**, *9*, 119.

0020-1669/95/1334-4888$09.00/0

niobium(V) catecholato complexes without oxo ligands via a smooth axial ligand exchange and a concomitant and novel Nb=O bond cleavage reaction.

The inherent redox activity of catecholato ligands plays a central role in intermolecular electron transfer reactions. Bidentate catecholato complexes have been intensively investigated from the viewpoint of inner-sphere electron transfer activity. Recently, several studies on intramolecular cobalt-quinone electron transfer have been carried out.[13] Pierpont and co-workers have written review articles on the formation of semiquinone or quinone complexes from complexes of other metals with quinone ligands.[14] The structures of monodentate catecholato complexes were first determined by Que and co-workers.[15] In order to form bidentate catecholato complexes, the deprotonation of the monodentate catecholato ligand was performed by using a strong base, such as potassium *tert*-butoxide.[16]

Raymond et al. published the first definitive article about the displacement of the V=O bond of $VO(cat)_2^{2-}$ by catechol.[17] The displacement of the very stable V=O bond was highly dependent on the pH of the aqueous medium. They emphasized that the catecholato ligand has an exceptional chelating ability that can stabilize strong Lewis acid metal ions in a high oxidation state. In early transition metal porphyrins that had an oxo ligand at the axial site, the Ti=O bond of $Ti^{IV}O(tpp)$ was displaced by catechol to give $Ti^{IV}(cat)(tpp)$.[18] However, no other metal−oxo bond of an oxometalloporphyrin has been reported to be cleaved by catechol.

In this paper, we describe the synthesis and characterization of novel catecholato niobium(V) porphyrins including an X-ray crystallographic study of a complex having two distinct catecholato ligands that are linked through intramolecular hydrogen bonding. It is emphasized that the bidentate catecholato ligand is produced through a unique Nb=O cleavage route involving intramolecular hydrogen bonding and electron transfer, and not through deprotonation with a strong base. We also present our attempts to gain mechanistic insights into the catechol coordination to the niobium(V) center by using ^{1}H-NMR spectroscopy to detect reaction intermediates.

Experimental Section

Materials. H_2tpp (Tokyo Kasei) was used without further purification. H_2tmp was prepared according to the method of Lindsey et al.[19] Extra pure grade dichloromethane (Nacalai Tesque) was purified by fractional distillation. Guaranteed grade (Nacalai Tesque) hexane, acetone, methanol, and acetic acid were used as supplied. An extra pure grade catechol (Tokyo Kasei) and 3,5-di-*tert*-butylcatechol (Aldrich, 99%) were used without further purification.

Syntheses of Nb(tpp)(O)(AcO) (1) and Nb(tmp)(O)(AcO) (2). $\{Nb(tpp)\}_2O_3$ and $\{Nb(tmp)\}_2O_3$ were prepared as previously described by employing H_2tpp and H_2tmp[1,4] and characterized by UV−vis absorption, IR, and ^{1}H-NMR spectroscopies. $\{Nb(tpp)\}_2O_3$ (0.21 g, 0.14 mmol) was dissolved in a mixture (20 mL) of benzene and acetic acid (1:1 v/v) and refluxed for 5 h. The solution was stored at room temperature, and purple crystals were isolated by evaporation of benzene; yield 0.23 g (97%). Anal. Calcd for Nb(tpp)(O)(AcO)·AcOH: C, 68.57; H, 4.20; N, 6.66. Found: C, 68.33; H, 4.16; N, 6.60. ^{1}H-NMR ($CDCl_3$, −50 °C): δ = 9.08 (s, pyrrole, 8H), 8.42 and 8.07 (m, *o*-phenyl, 8H), 7.78−7.85 (m, *m,p*-phenyl, 12H), 0.43 (s, CH_3-COO, 3H), and 2.15 (s, CH_3COOH as the crystal solvent, 3H). Electronic spectrum (benzene): 429 (log ϵ = 5.70), 532 (4.08), and 554 (4.25) nm. IR (KBr): ν(Nb=O) 908 cm^{-1}.

Nb(tmp)(O)(AcO) was prepared in the same way; yield 92%. Anal. Calcd for Nb(tmp)(O)(AcO)·AcOH: C, 71.42; H, 5.89; N, 5.55. Found: C, 71.62; H, 5.89; N, 5.27. ^{1}H-NMR ($CDCl_3$, room temperature): δ = 8.84 (s, pyrrole, 8H), 7.35 and 7.23 (s, *m*-mesityl, H, 8H), 2.63 (s, *p*-mesityl, CH_3, 12H), 2.20 and 1.57 (s, *o*-mesityl, CH_3, 24H), 0.35 (bs, CH_3COO, 3H), and 2.08 (bs, CH_3COOH as the crystal solvent, 3H). Electronic spectrum (benzene): 431 (log ϵ = 5.70), 534 (4.07), and 556 (4.22) nm. IR (KBr): ν(Nb=O) 905 cm^{-1}.

Syntheses of Nb(tpp)(cat)(Hcat) (3), Nb(tmp)(cat)(Hcat) (4), and Nb(tpp)(dbc)(Hdbc) (5). Nb(tpp)(O)(AcO)·AcOH (0.20 g, 0.24 mmol) and an excess amount of catechol (0.30 g, 2.7 mmol) were dissolved in a mixture (40 mL) of dichloromethane and hexane (1:1 v/v). The dark red solution was stored in a refrigerator (2 °C) until the solution turned colorless and **3** was precipitated as dark purple crystals. The cured product, which contained unreacted catechol, was washed with acetone to remove the contaminating catechol and recrystallized from a mixture (40 mL) of dichloromethane and hexane (1:1 v/v) in a refrigerator (2 °C) under slow evaporation of solvent; yield 0.24 g (98%). Anal. Calcd for Nb(tpp)(cat)(Hcat)·$^1/_2C_6H_{14}$·CH_2Cl_2: C, 68.58; H, 4.41; N, 5.33. Found: C, 68.63; H, 4.50; N, 5.27. The presence of hexane and dichloromethane in the crystals were confirmed by ^{1}H-NMR spectroscopy. Electronic spectrum (benzene): 419 (log ϵ = 5.25), and 544 (4.25) nm. IR (KBr): ν(C−O in bidentate cat ligand); 1256 cm^{-1}.

Nb(tmp)(cat)(Hcat) was prepared similarly; yield 90%. Anal. Calcd for Nb(tmp)(cat)(Hcat)·$^1/_2C_6H_{14}$: C, 75.18; H, 6.04; N, 4.94. Found: C, 74.90; H, 6.26; N, 4.68. Electronic spectrum (benzene): 422 (log ϵ = 5.20), and 540 (4.21) nm. IR (KBr): ν(C−O in bidentate cat ligand) 1261 cm^{-1}.

Nb(tpp)(dbc)(Hdbc) was prepared by the same method used to prepare complexes **3** and **4** by using 3,5-di-*tert*-butylcatechol in place of catechol; yield 82%. Anal. Calcd for Nb(tpp)(dbc)(Hdbc)·$^1/_2CH_2Cl_2$·$^1/_2C_6H_{14}$: C, 73.56; H, 6.30; N, 4.54. Found: C, 74.08; H, 6.29; N, 4.56. Electronic spectrum (benzene): 416 (log ϵ = 5.21), and 545 (4.31) nm. IR (KBr): ν(C−O in bidentate dbc ligand) 1304 cm^{-1}.

Instrumentation. UV−vis absorption and IR spectra were recorded on a Jasco Ubest-55 UV/VIS spectrophotometer and a Shimadzu FTIR-8600 instrument, respectively. ^{1}H-NMR spectra were measured by a JEOL GX-400 or a GSX-400.

X-ray Crystallographic Study of Nb(tpp)(cat)(Hcat) (3). The recrystallization of crude Nb(tpp)(cat)(Hcat) from hexane/dichloromethane (1:1 v/v), under slow evaporation of solvent at 2 °C, resulted in the formation of dark purple crystals that were suitable for X-ray crystallography. The water in the unit cell was derived from soluble water in the dichloromethane that was introduced from moisture or by the displacement of the oxo ligand of **1**. The crystal was mounted in a glass capillary. All measurements were performed with a Rigaku AFC7R diffractometer with a 12 kW rotating anode generator. Cell constants and an orientation matrix were obtained from a least-squares refinement using 25 reflections in the range 36.35° < 2θ < 40.06°. Data were collected with the ω−2θ scan technique. The intensities of three reflections were monitored after every 150 reflections and no decay correction was applied. Both empirical and Lorenz-polarization absorption corrections were made. The crystallographic data are presented in Table 1. Selected atomic positional parameters are given in Table 2.

All the calculations were performed with the teXsan crystallographic software package (Molecular Structure Corp.). The structure was solved by the Patterson method.[20] The positions of some of the non-hydrogen atoms (dichloromethane and the water molecule of crystallization) were refined isotropically, while the positions of the others were refined

(13) (a) Buchanan, R. M.; Pierpont, C. G. *J. Am. Chem. Soc.* **1980**, *102*, 4951. (b) Adams, D. M.; Dei, A.; Rheingold, A. L.; Hendrickson, D. N. *J. Am. Chem. Soc.* **1993**, *115*, 8221. (c) Jung, O.-S.; Pierpont, C. G. *Inorg. Chem.* **1994**, *33*, 2227.
(14) (a) Pierpont, C. G.; Buchanan, R. M. *Coord. Chem. Rev.* **1981**, *38*, 45. (b) Pierpont, C. G.; Lange, C. W. Prog. *Inorg. Chem.* **1994**, *41*, 331.
(15) Heistand II, R. H.; Roe, A. L.; Que, L., Jr. *Inorg. Chem.* **1982**, *21*, 676.
(16) Heistand II, R. H.; Lauffer, R. B.; Fikrig, E.; Que, L., Jr. *J. Am. Chem. Soc.* **1982**, *104*, 2789.
(17) Cooper, S. R.; Koh, Y. B.; Raymond, K. N. *J. Am. Chem. Soc.* **1982**, *104*, 5092.
(18) (a) Deronzier, A.; Latour, J. M. *Nouv. J. Chim.* **1984**, *8*, 393. (b) Marchon, J.-C.; Latour, J.-M.; Grand, A.; Belakhovsky, M.; Loos, M.; Goulon, J. *Inorg. Chem.* **1990**, *29*, 57.
(19) Lindsey, J. S.; Schreiman, I. C.; Hsu, H. C.; Kearney, P. C.; Marguerettaz, A. M. *J. Org. Chem.* **1987**, *52*, 827.

Table 1. Crystallographic Data and Computation for Nb(tpp)(cat)(Hcat)·CH_2Cl_2·H_2O

formula	$C_{57}H_{41}N_4O_5Cl_2Nb$	Z	4
fw	1025.79	T, K	293
space group	$P2_1/c$	ϱ_{calc}, g·cm^{-3}	1.406
a, Å	14.592(3)	radiation (λ, Å)	Mo Kα (0.710 69)
b, Å	23.457(10)	μ, cm^{-1}	4.13
c, Å	14.415(4)	GOF	5.87
β, deg	100.95(2)	R[a]	0.079
V, Å^3	4844(2)	R_w[b]	0.093

[a] $R = \sum||F_o| - |F_c||/\sum|F_o|$. [b] $R_w = [(\sum w(|F_o| - |F_c|)^2/\sum w(F_o)^2)]^{1/2}$.

Table 2. Selected Atom Coordinates for Nb(tpp)(cat)(Hcat)

	x	y	z	B_{eq}, Å^2
Nb(1)	0.26029(7)	0.12923(4)	−0.04821(7)	2.92(2)
O(1)	0.2787(4)	0.1639(3)	−0.1785(5)	3.3(2)
O(2)	0.1495(4)	0.1769(3)	−0.0888(4)	3.2(2)
O(3)	0.3300(5)	0.1942(3)	−0.0003(5)	3.6(2)
O(4)	0.4186(5)	0.2427(4)	−0.1341(6)	5.6(2)
N(1)	0.1522(5)	0.0966(3)	0.0279(5)	2.9(2)
N(2)	0.3432(5)	0.1014(4)	0.0946(5)	3.0(2)
N(3)	0.3792(5)	0.0829(3)	−0.0875(6)	3.0(2)
N(4)	0.1870(5)	0.0668(3)	−0.1520(5)	3.0(2)
C(1)	0.0597(7)	0.0918(5)	−0.0191(7)	3.1(3)
C(2)	−0.0017(7)	0.1007(5)	0.0462(7)	3.5(3)
C(3)	0.0525(7)	0.1062(5)	0.1319(8)	3.9(3)
C(4)	0.1497(7)	0.1035(4)	0.1226(7)	3.1(3)
C(5)	0.2244(7)	0.1060(4)	0.1973(7)	3.3(3)
C(6)	0.3144(7)	0.1018(4)	0.1815(7)	3.4(3)
C(7)	0.3957(8)	0.1003(5)	0.2576(7)	4.5(3)
C(8)	0.4729(7)	0.1010(5)	0.2181(8)	4.3(3)
C(9)	0.4400(7)	0.1016(4)	0.1177(7)	3.3(3)
C(10)	0.4990(7)	0.1034(5)	0.0515(8)	3.4(3)
C(11)	0.4719(7)	0.0930(4)	−0.0425(7)	3.1(3)
C(12)	0.5312(7)	0.0814(5)	−0.1078(8)	4.1(3)
C(13)	0.4786(7)	0.0627(5)	−0.1879(7)	4.0(3)
C(14)	0.3831(7)	0.0641(5)	−0.1783(7)	3.1(3)
C(15)	0.3091(7)	0.0468(5)	−0.2433(7)	3.2(3)
C(16)	0.2176(7)	0.0466(4)	−0.2304(7)	3.3(3)
C(17)	0.1383(8)	0.0259(5)	−0.2984(8)	4.2(3)
C(18)	0.0610(7)	0.0346(5)	−0.2620(8)	4.2(3)
C(19)	0.0897(7)	0.0602(5)	−0.1719(7)	3.3(3)
C(20)	0.0300(7)	0.0758(4)	−0.1113(7)	3.0(3)
C(45)	0.2061(7)	0.1926(4)	−0.2268(8)	3.2(3)
C(46)	0.1972(8)	0.2131(5)	−0.3157(8)	4.1(3)
C(47)	0.1192(10)	0.2446(5)	−0.3551(8)	5.2(4)
C(48)	0.0442(9)	0.2537(5)	−0.3078(9)	5.4(4)
C(49)	0.0513(8)	0.2305(5)	−0.2182(9)	4.6(3)
C(50)	0.1331(8)	0.1998(5)	−0.1760(8)	3.9(3)
C(51)	0.3966(7)	0.2344(5)	0.0265(8)	3.7(3)
C(52)	0.4242(9)	0.2533(6)	0.1195(8)	4.9(4)
C(53)	0.4935(9)	0.2972(6)	0.1423(10)	5.9(4)
C(54)	0.5330(10)	0.3198(6)	0.079(1)	6.8(5)
C(55)	0.5109(9)	0.3026(6)	−0.016(1)	6.1(4)
C(56)	0.4422(9)	0.2613(5)	−0.0427(9)	4.7(4)

anisotropically. Hydrogen atoms were placed in idealized positions (d(C−H) = 0.95 Å) and not refined. Refinement was carried out by using full-matrix least-squares techniques with scattering factors[21] and anomalous dispersion terms.[22] The values of $\Delta f'$ and $\Delta f''$ were those of Creagh and McAuley.[23] The residual maximum peak on the final difference Fourier map was found with 1.13 e/Å^3 near an oxygen atom of the water molecule of crystallization. Final atomic coordinates and anisotropic thermal factors can be found in the supplementary material.

Results and Discussion

Syntheses of Niobium(V)porphyrins. {Nb(tmp)}$_2$O$_3$ could be prepared by the same method used to prepare {Nb(tpp)}$_2$O$_3$, *i.e.*, $NbCl_5$ was used to insert the niobium into H_2tmp in place of H_2tpp. The metal insertion into H_2tmp required a fairly long time, about 30 h, while the metalation of H_2tpp was completed in 3 h. The obtained {Nb(tmp)}$_2$O$_3$ appeared to have the same structure as that of the tris(μ-oxo) dimer of {Nb(tpp)}$_2$O$_3$ on the basis of its ^{1}H-NMR and IR spectra and elemental analysis.[24] Previously, acetato complexes were prepared by dissolving the tris(μ-oxo) dimer into hot acetic acid, but this method was always accompanied by the demetalation of the porphyrin ligand.[4] On the other hand, in the present modified method as described in the experimental section, the acetato complexes were quantitatively isolated from a benzene−acetic acid (1:1 v/v) solution of tris(μ-oxo) dimers without demetalation. Crude catecholato complexes were easily obtained by mixing the corresponding acetato complex and the excess amount of catechol in dichloromethane−hexane at room temperature, followed by recrystallization from dichloromethane−hexane (1:1 v/v). The catecholato complex prepared in this way was no longer subject to hydrolysis to form the tris(μ-oxo) dimer, although phenolato or alkolato complexes were easily hydrolyzed, and therefore, difficult to isolate.[10] The resistance of the catecholato complex to hydrolysis is attributable to the stabilization due to the chelating effect of the bidentate catecholato ligand and to intramolecular hydrogen bonding of the monodentate catecholato ligand. It is notable that we can obtain the catecholato complex even with the bulkier tmp skeleton. It should be emphasized that the tmp complex also has a sufficiently large cavity to bind two catecholato ligands, as mentioned below. However, the yield of Nb(tmp)(cat)(Hcat) was somewhat lower than that of Nb(tpp)(cat)(Hcat), and the preparation was somewhat troublesome because the reaction solution was contaminated with unidentified impurities.

Molecular Structure of Nb(tpp)(cat)(Hcat) (3). Figure 1 shows a top view (A) and side view (B) of the Nb(tpp)(cat)(Hcat) (**3**) molecule, and also shows the numbering of the coordinating atoms. The molecule clearly contains two nonequivalent catechols. One catechol is a dianion acting as a bidentate ligand and the other is a monoanion acting as a monodentate ligand. The two catechol ligands are located on the same side of the porphyrin plane. The molecule ultimately preferred a heptacoordinate and *cis*-configured structure. This is similar to other niobium(V)porphyrins, such as {Nb(tpp)}$_2$O$_3$[4,7] and Nb(tpp)(O)(AcO).[3,4] In this manner, d^0 metal porphyrins show a strong preference for the *cis*-configuration.[25] Zirconium(IV)porphyrins also contain a d^0 ion as a central metal. The molecular structures of (μ-O)(μ-OH)$_2${Zr(tpp)}$_2$[26] and Zr(oep)(CH_2SiMe_3)$_2$[27] have been confirmed by X-ray crystallography to have the *cis*-configuration.

(20) DIRDIF92: Beurskens P. T.; Admiraal, G.; Beurkens, G.; Bosman, W. P.; Gracia-Granda, S.; Gould, R. O.; Smits, J. M. M.; Smykalla, C. The DIRDIF program system, Technical report of the Crystallography Laboratory, University of Nijmegen, the Netherlands, 1992.
(21) Cromer, D. T.; Waber, J. T. *International Tables for X-ray Crystallography*; Kynoch Press: Birmingham, England, 1974; Vol. IV, Table 2.2 A.
(22) Ibers, J. A.; Hamilton, W. C. *Acta. Crystallogr.* **1964**, *17*, 781.
(23) Creagh, D. C.; McAuley, W. J. *International Tables for Crystallography*; Wilson, A. J. C., Ed.; Kluwer Academic Publishers: Boston, MA, 1992; Vol. C, Table 4.2.6.8.
(24) Anal. Calcd for {Nb(tmp)}$_2$O$_3$: C, 74.90; H, 5.84; N, 6.24. Found: C, 75.02; H, 6.04; N, 6.04. A strong IR band assigned to the Nb=O stretch was not observed. ^{1}H-NMR ($CDCl_3$, room temperature): δ = 8.08 (s, pyrrole, 8H), 7.30 and 6.93 (s, *o*-mesityl, H, 8H), 2.58 (s, *p*-mesityl, CH_3, 12H), 1.67 and 0.82 (s, *o*-mesityl, CH_3, 24H). This complex shows a significant high field shift for the signal of pyrrole protons compared with monomeric complexes, such as Nb(tpp)(O)(AcO) and Nb(tmp)(O)(AcO). This feature is quite characteristic of dimeric niobium(V) porphyrins. The high field shift is similer to that of {Nb(tpp)}$_2$O$_3$ (8.39 ppm) and results from the shielding effect of the ring current of another porphyrin moiety in the dimeric complexes.
(25) Gouterman, M.; Hanson, L. K.; Khalil, G.-E.; Buchler, J. W.; Rohbock, K.; Dolphin, D. *J. Am. Chem. Soc.* **1975**, *97*, 3142.
(26) Kim, H.-J.; Whang, D.; Do, Y.; Kim, K. *Chem. Lett.* **1993**, 807.
(27) Brand, H.; Arnold, J. *J. Am. Chem. Soc.* **1992**, *114*, 2266.

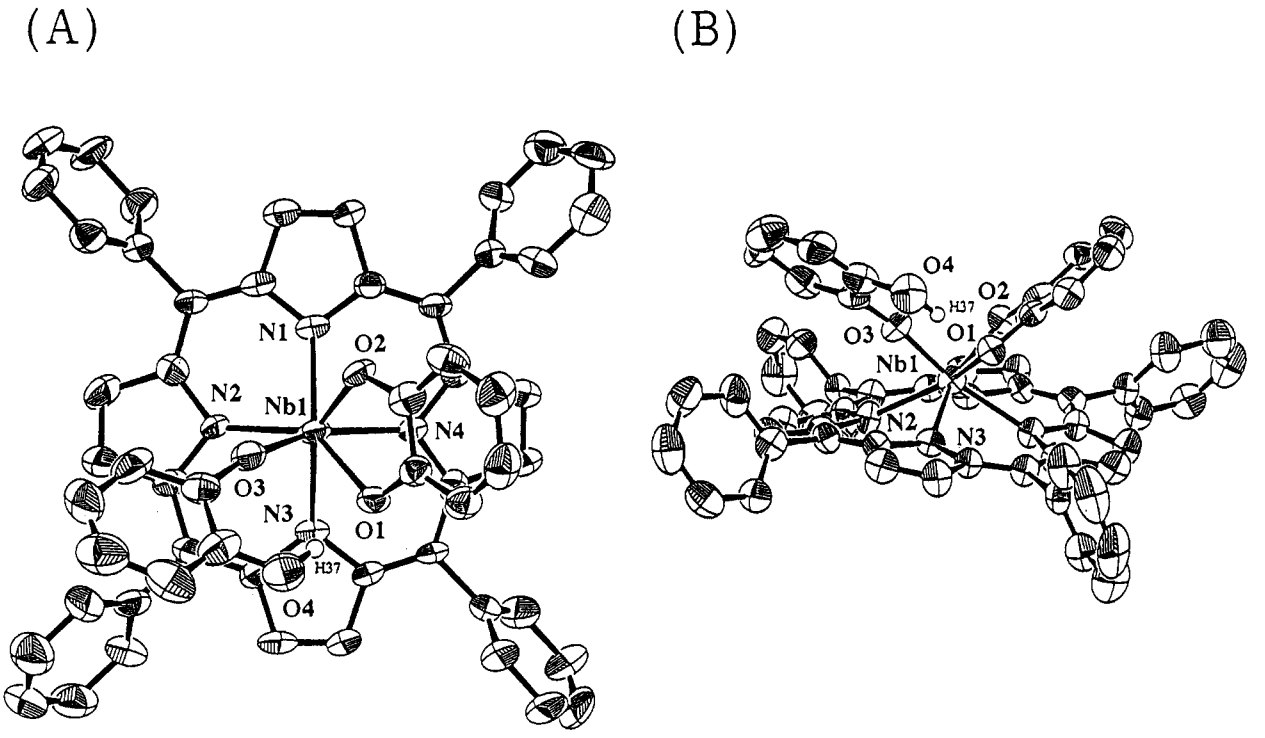

Figure 1. Molecular structure of Nb(tpp)(cat)(Hcat) (**3**): A, top view; B, side view. Coordinates of labeled atoms are given in Table 2.

Table 3. Selected Interatomic Distances and Bond Angles in Complex **3**

	(a) Interatomic Distances (Å)		
Nb–O(1)	2.110(6)	Nb–O(2)	1.961(7)
Nb–O(3)	1.888(7)	Nb–N(1)	2.220(7)
Nb–N(2)	2.276(8)	Nb–N(3)	2.209(7)
Nb–N(4)	2.218(8)	O(1)–C(45)	1.33(1)
O(2)–C(50)	1.35(1)	O(3)–C(51)	1.36(1)
O(4)–C(56)	1.37(1)	C(45)–C(46)	1.35(1)
C(45)–C(50)	1.41(1)	C(46)–C(47)	1.39(1)
C(47)–C(48)	1.41(2)	C(48)–C(49)	1.39(2)
C(49)–C(50)	1.43(1)	C(51)–C(52)	1.40(1)
C(51)–C(56)	1.45(1)	C(52)–C(53)	1.44(2)
C(53)–C(54)	1.28(2)	C(54)–C(55)	1.41(2)
C(55)–C(56)	1.39(2)		
	(b) Bond Angles (deg)		
O(1)–Nb–O(2)	75.6(3)	O(1)–Nb–O(3)	82.2(3)
O(1)–Nb–N(1)	142.6(3)	O(1)–Nb–N(2)	141.3(3)
O(1)–Nb–N(3)	73.9(3)	O(1)–Nb–N(4)	77.3(3)
O(2)–Nb–O(3)	90.3(3)	O(2)–Nb–N(1)	73.8(3)
O(2)–Nb–N(2)	134.4(3)	O(2)–Nb–N(3)	147.8(3)
O(2)–Nb–N(4)	84.9(3)	O(3)–Nb–N(1)	118.7(3)
O(3)–Nb–N(2)	75.2(3)	O(3)–Nb–N(3)	95.5(3)
O(3)–Nb–N(4)	159.5(3)	N(1)–Nb–N(2)	76.1(3)
N(1)–Nb–N(3)	128.5(3)	N(1)–Nb–N(4)	79.0(3)
N(2)–Nb–N(3)	77.4(3)	N(2)–Nb–N(4)	121.7(3)
N(3)–Nb–N(4)	78.7(3)	Nb–O(1)–C(45)	115.9(6)
Nb–O(2)–C(50)	119.8(6)	Nb–O(3)–C(51)	166.3(7)
Nb–N(1)–C(1)	120.0(6)	Nb–N(1)–C(4)	127.1(7)
Nb–N(2)–C(6)	127.7(7)	Nb–N(2)–C(9)	123.9(6)
Nb–N(3)–C(11)	122.3(6)	Nb–N(3)–C(14)	124.8(7)
Nb–N(4)–C(16)	126.3(6)	Nb–N(4)–C(19)	123.3(6)

Table 3 gives the selected bond distances and angles of the Nb(tpp)(cat)(Hcat) molecule. It shows clearly that O(1)–O(3) coordinate to the niobium atom while O(4) is located far from the niobium atom. In other words, one catecholato moiety acts as a bidentate ligand and the other acts as a monodentate ligand. The two Nb–O distances of the bidentate catechol are slightly different. In the solid state, the bidentate catechol asymmetrically ligates to the niobium atom due to the intramolecular hydrogen bonding of an uncoordinated OH group to O(1). The interatomic distance between the coordinated oxygen atom O(1) of the bidentate catechol and O(4) of the uncoordinated OH group of the monodentate catechol was 2.74 Å, which was close enough to form an intramolecular hydrogen bond.[28] This hydrogen bonding weakens the Nb–O(1) interaction and make the Nb–O(1) bond distance longer than that of Nb–O(2). Of the three Nb–O bond lengths, Nb–O(3) of the monodentate catechol is the shortest (1.887(7) Å), the hydrogen-bonded Nb–O(1) is the longest (2.110(6) Å), and the Nb–O(2) of the bidentate catechol is intermediate (1.961(7) Å). In addition, these Nb–O single bond distances are comparable to those observed in Nb(tpp)(O)(AcO) (2.22 Å for chelating acetato ligand)[3,4] and the tris(μ-oxo) dimer, $\{Nb(tpp)\}_2O_3$ (1.81–1.91 Å).[4] The four individual Nb–N distances are essentially all equivalent with an average value of 2.231 Å. A similar result was described in the case of $\{Nb(tpp)\}_2O_3$.[4] In contrast, the Nb–N distances of Nb(tpp)(O)(AcO) are considerably different from each other, because the Nb–N bonds are influenced by a strong Nb=O bond.[3,4] The niobium ion in Nb(tpp)(cat)(Hcat) is displaced 1.02 Å from the plane of the four porphinate nitrogen atoms. This displacement value is similar to the 1.02 Å for $\{Nb(tpp)\}_2O_3$,[4] and the 1.00 Å for Nb(tpp)(O)(AcO)[3,4] and Nb(oep)(O)(F).[8] These observations indicate that similar steric distortions can be observed in hexa- or heptacoordinate niobium(V) porphyrin complexes. The bidentate catechol ligand is located above one pyrrole ring and interatomic distances between the α-carbons of the pyrrole moiety and the carbons bound to oxygen atoms in the catechol are 3.43 and 3.34 Å, respectively, which are close enough to form a π–π interaction to stabilize this structure. All the C–O bond lengths of Nb(tpp)(cat)(Hcat) fall into the range 1.33–1.37 Å, which is typical of C–O single bonds in catechols, but too long to be C–O bonds in semiquinonato ligands (Table 4). As will be discussed later, IR spectra of **3** and **4** also suggest no semiquinone character. Furthermore, a variable-temperature ESR study did

(28) (a) Borgias, B. A.; Cooper, S. R.; Koh, Y. B.; Raymond, K. N. *Inorg. Chem.* **1984**, *23*, 1009. (b) Zirong, D.; Bhattacharya, S.; McCusker, J. K.; Hagen, P. M.; Hendrickson, D. N.; Pierpont, C. G. *Inorg. Chem.* **1992**, *31*, 870.

Table 4. C−O Bond Lengths and Stretching Frequencies of Catecholate, Quinone, and Semiquinone Ligands

complex	C−O, Å	ν(C−O), cm^{-1}	ref
Nb(tpp)(cat)(Hcat)	1.33−1.37	1256	this work
Nb(tmp)(cat)(Hcat)		1261	this work
Nb(tpp)(dbc)(Hdbc)		1304	this work
$[(CH_3)_4N]^+[ReO(cat)_2(PPh_3)]^-$	1.333−1.380	1237	29
trans-Ru(dbq)$_3$[b]	1.28−1.34	1155	30
trans-Os(dbq)$_3$[b]	1.32−1.35	1158	30
Fe(dbsq)$_3$[b]	1.276−1.287	1480	*a*, 30

[a] Boone, S. R.; Purser, G. H.; Chang, H.-R.; Lowery, M. D.; Hendrickson, D. N.; Pierpont, C. G. *J. Am. Chem. Soc.* **1989**, *111*, 2292. [b] dbq and dbsq denote 3,5-di-*tert*-butylbenzoquinone and 3,5-di-*tert*-butylsemiquinone, respectively.

not show any temperature-dependent catechol−semiquinone tautomerization due to intramolecular electron transfer in the range 300−77 K, unlike complexes reported by Pierpont, Hendrickson, and co-workers.[13]

Spectroscopic Properties of Catecholato Complexes. IR spectra of Nb^V(porphyrin)(cat)(Hcat) complexes showed a strong absorption due to ν(C−O) of the catecholato ligands. For **3**, the absorption was observed at 1256 cm^{-1} and for **4** it was observed at 1261 cm^{-1}. Both of these wavenumbers are close to the typical range of catechol ν(C−O) (1235−1250 cm^{-1})[29] and indicate that the catecholato ligands studied have no semiquinone character, for which the ν(C−O) would be observed around 1500 cm^{-1}.[30]

In order to understand the solution structures of catecholato complexes, ^{1}H-NMR spectroscopy was employed. Peak assignments were made by peak integration, multiplicity, and deuterium substitution.

The addition of 2 equiv of catechol to the $CDCl_3$ solution of **1** forms complex **3** as mentioned above. This reaction drastically changed the spectrum to show additional broad signals due to metal-bound catechols in the range from 4.0 to 6.5 ppm, which was different from that of free catechol. At −50 °C, the broad signals were clearly resolved to show multiplicity, as shown in Figure 2. The assignments are listed in Table 5 and the labeling scheme for catecholato ligands is given in Figure 3. An eight-proton singlet observed at 9.03 ppm was assigned to the pyrrole protons of tpp, which was slightly shifted from that of **1**. It is intriguing that the signal of the pyrrole proton can be observed as a singlet even at −50 °C.[18a,31] Two multiplets observed at 5.18 and 6.00 ppm are assigned to protons **a** and **b** of bidentate catechol. This suggests that the bidentate catechol moiety has a symmetrical plane and that, in solution, the intramolecular hydrogen bonding between the uncoordinated hydroxyl group of the monodentate catechol and the bidentate catechol is delocalized between two coordinating oxygen atoms of the bidentate catechol. The symmetry of the bidentate catecholato ligand indicates that the monodentate catecholato ligand is perpendicular relative to the bidentate one. Two similar multiplets of bidentate catechols have been observed in crystallographically characterized $[Re(O)(cat)_2]^-$.[29] Concerning

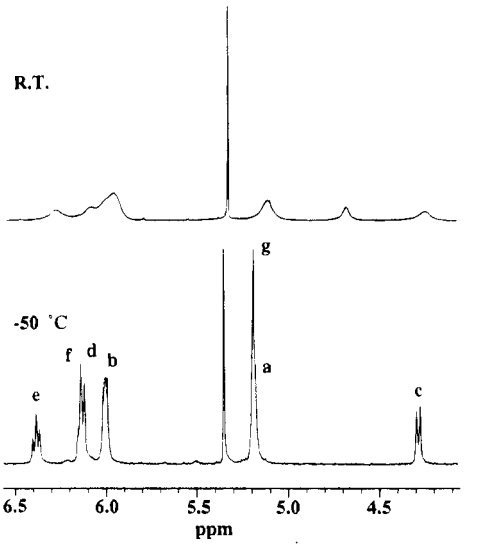

Figure 2. ^{1}H-NMR spectra of **3** in the region of catecholato ligands in $CDCl_3$ at room temperature (top) and −50 °C (bottom). Peak assignments are given in Table 5. Protons belonging to cat and Hcat are labeled as shown in Figure 3.

Table 5. Peak Assignments for ^{1}H-NMR Data of the Complex **3** and **4**[a]

chem shift (ppm)[b]		intg, mult (*J*, Hz)		assignment[c]	
3	**4**	**3**	**4**	**3**	**4**
	1.56		nd,[f] s		*o*-Me[d]
	2.11		12H, s		*o*-Me[e]
	2.61		12H, s		*p*-Me
5.18	4.64	2H, m	2H, m	**a**	**a**
6.00	5.52	2H, m	2H, m	**b**	**b**
4.28	3.86	1H, d (8.3)	1H, dd (1.5, 8.3)	**c**	**c**
6.14	5.54	*g*	1H, td (1.5, 7.8)	**d**	**d**
6.39	5.75	1H, t (7.8)	1H, td (1.5, 7.8)	**e**	**e**
6.13	5.64	*g*	1H, dd (1.5, 8.0)	**f**	**f**
5.21	3.64	1H, s	1H, s	**g**	**g**
	7.22		4H, s		*m*-H[d]
	7.31		4H, s		*m*-H[e]
7.81		12H, m		*m, p*-H	
7.96		4H, d (7.3)		*o*-H[d]	
8.07		4H, d (7.8)		*o*-H[e]	
9.03	8.84	8H, s	8H, s	pyrrole H	pyrrole H

[a] Measured in $CDCl_3$ at −50 °C. [b] TMS as a reference. [c] Protons belonged to cat and Hcat ligands were labeled as shown in Figure 3. [d] Located on the opposite side with respect to the axial ligands. [e] Located on the same side with respect to the axial ligands. [f] Overlapped with H_2O peak. [g] Integration intensity for both corresponded to two protons. Coupling constants were not able to be determined because of their overlapping.

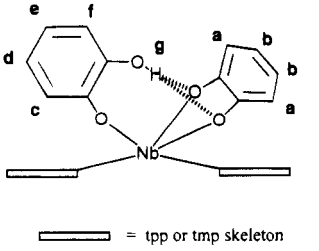

Figure 3. Labeling scheme for **3** or **4**.

the monodentate catechol ligand, the four protons are all inequivalent, and therefore, show four resonances. Their chemical shifts were essentially affected by their relative distances from the porphyrin plane. Proton **c**, which shows a doublet signal, is closest to the ring, and therefore shifts the resonance at the highest field, 4.28 ppm to show a doublet.

(29) Kettler, P. B.; Chang, Y.-D.; Zubieta, J.; Abrams, M. J. *Inorg. Chim. Acta* **1994**, *218*, 157.

(30) (a) Cass, M. E.; Gordon, N. R.; Pierpont, C. G. *Inorg. Chem.* **1986**, *25*, 3962. (b) Bhattacharya, S.; Boone, S. R.; Fox, G. A.; Pierpont, C. G. *J. Am. Chem. Soc.* **1990**, *112*, 1088. (c) Bhattacharya, S.; Pierpont, C. G. *Inorg. Chem.* **1992**, *31*, 35.

(31) Essentially, if the orientations of axial ligands are fixed relative to the porphyrin ring, the presence of the axial ligands must induce a dissymmetry for pyrrole protons. In niobium(V) porphyrins, one narrow signal due to pyrrole protons is regarded as pseudorotation of the axial ligands: Tachibana, J.; Imamura,T.; Sasaki,Y. *J. Chem. Soc., Chem. Commun.* **1993**, 1436.

Table 6. Peak Assignments for ^{1}H-NMR Data of Complex **5**

chemical shift (ppm)[a]			
−50 °C	room temp	intg, mult (*J*, Hz)[b]	assignment[c]
0.18	0.21	9H, s	tBu(1)
0.71	0.69	9H, s	tBu(2)
0.90	0.91	9H, s	tBu(4)
1.20	1.09	9H, s	tBu(3)
5.02	4.92	1H, d (2.0)	**a**
5.61	5.63	1H, d (2.0)	**b**
4.24	3.99	1H, d (2.3)	**c**
6.58	6.43	1H, d (2.3)	**d**
3.84	3.60	1H, s	**e**
7.88	7.72	16H, m	*o*, *m*, *p*-H
8.08	7.97	4H, s	*o*′-H
8.92	8.91	8H, s	pyr-*β*-H

[a] Measured in $CDCl_3$ with TMS as a reference. [b] Data at −50 °C. [c] Protons belonged to dbc and Hdbc ligands were labeled as shown in Figure 4.

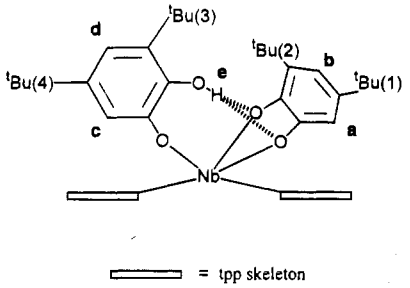

Figure 4. Labeling scheme of **5**.

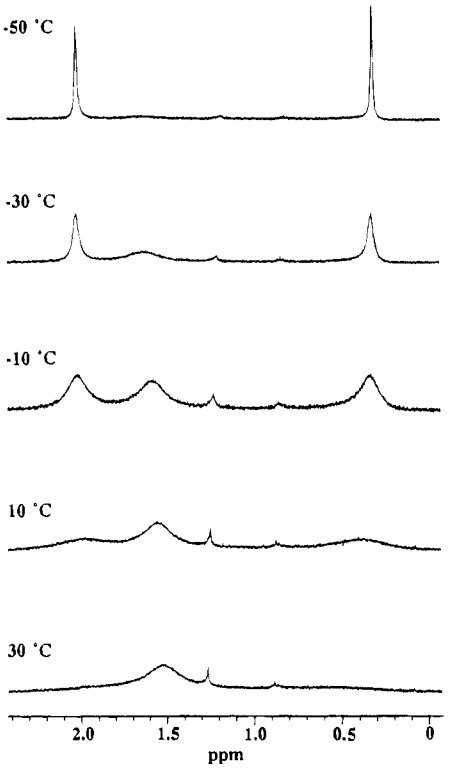

Figure 5. Temperature dependence of the ^{1}H-NMR spectrum of **1** in CD_2Cl_2 in the region of the acetato ligand.

Proton **e** is the least shielded, and, thus it resonates as a triplet at the lowest field, 6.39 ppm. Peaks due to protons **d** and **f** appear at 6.14 ppm as a triplet and at 6.13 ppm as a doublet, respectively. The resonance due to proton **g** of the uncoordinated hydroxyl group of the monodentate catechol could easily be assigned to that at 5.21 ppm because it diminishes upon addition of aliquots of D_2O.

When tmp was used in place of tpp, in sharp contrast to **3**, complex **4** showed a well-resolved ^{1}H-NMR spectrum in $CDCl_3$, even at room temperature. Peak assignments are given in Table 5. As for the catecholato moiety of **4**, it showed a signal pattern that was similar to that of **3**. Two multiplets at 4.64 and 5.52 ppm were assigned to protons of the bidentate catecholato ligand (protons **a** and **b**). The assignment was unambiguously confirmed by two-dimensional ^{1}H−^{1}H COSY and *J*-resolved spectra in $CDCl_3$. These observations suggest that the structure of **4** is the same as that of **3**, which was determined by X-ray analysis. The peak assignments (at −50 °C) for the complex **5**, which contains 3,5-di-*tert*-butylcatecholato ligands (dbc, Hdbc), are listed in Table 6 and the labeling scheme is given in Figure 4. ^{1}H-NMR and ^{1}H−^{1}H COSY spectra of **5** suggest that the structure of **5** is similar to those of **3** and **4**.

Reaction Mechanism of Nb=O Bond Cleavage and Catechol Coordination. Examination of the temperature dependence of the ^{1}H-NMR spectrum of the acetato complex **1** suggested the existence of a dissociation equilibrium for the acetato ligand. As shown in Figure 5, a broad signal at around 1.5 ppm at 30 °C gradually separated into two sharp singlets at 0.32 and 2.04 ppm as the temperature was lowered. One singlet at 2.04 ppm fully coincided with that of free acetic acid, and was attributed to acetic acid that was contained in the unit cell as a solvent of crystallization. The other singlet at 0.32 ppm was attributed to a coordinated acetato ligand and was shifted to a significantly higher field than that of free acetic acid by the strong shielding effect of the porphyrin ring current. At ambient temperature, two acetates, one coordinated and the other uncoordinated, were exchanged, and therefore were observed as one broad signal, whereas these two acetates were exchanged in a zone that was weakly shielded by the porphyrin ring current because the signal was detected at a slightly higher field than that of free acetic acid. This observation suggests the ionic dissociation of the acetato ligand. In the acetato complex **2** with the tmp skeleton, chemical exchange of the coordinated and uncoordinated acetates was very slow, even at ambient temperature, because the bulky mesityl groups disturbed the approach of the acetates to the metal center.

The decreased rate of the axial ligand exchange in the complex **2** was very helpful for following the reaction mechanisms of the Nb=O bond cleavage and coordination of catechol. As expected, two reaction intermediates were successfully detected by employing **2**, although the reaction of **1** with catechol was too fast to detect any intermediates. The change with time in the ^{1}H-NMR spectrum of the reaction mixture of **2** and 2 equiv of catechol in $CDCl_3$ at −30 °C was followed as shown in Figure 6. Three multiplet pairs derived from a bidentate catechol were observed during the course of the reaction. The pair labeled "**A**" (peaks at 4.94 and 5.83 ppm) is attributable to the **A** intermediate in the Scheme 1, and the pair labeled "**B**" (5.17 and 5.97 ppm) is attributable to the **B** intermediate. Both **A** and **B** possess a bidentate catechol. The residual multiplets pair at 4.64 and 5.52 ppm, as mentioned above, are attributed to the final complex **4**. It should be emphasized that a new singlet emerged at −0.12 ppm and the signal could not be observed for a deuterated starting complex, Nb(tmp)(O)(CD_3COO). This signal is clearly associated with a coordinated acetato ligand that is different from the one possessed by the starting complex **2** (0.35 ppm). The area under the peaks indicates that intermediate **B** possesses an axial acetato ligand (in addition to the bidentate catecholato ligand), whereas intermediate **A** does not. The ratio of the formation of **A** and **B** remained constant through the course of the reaction, but was dependent on the temperature. At −30 °C the ratio was approximately 1: 2, while at 23 °C it was 3:5. These

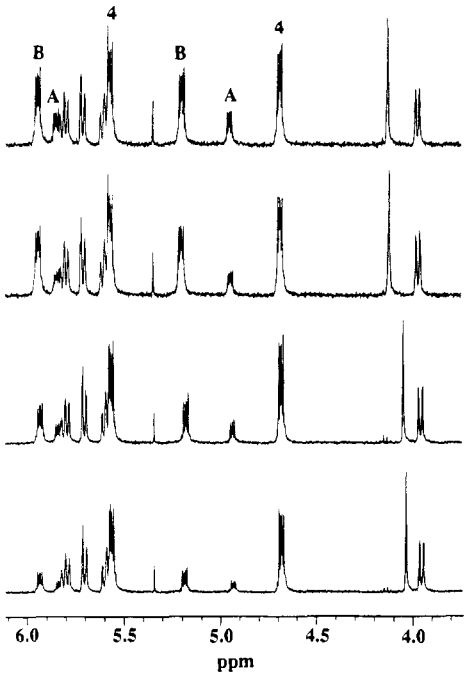

Figure 6. Time course of the ^{1}H-NMR spectrum of **2** in the region of catecholato ligands after addition of 2 equiv of catechol in $CDCl_3$ at −30 °C. Three labeled multiplet pairs correspond to intermediates **A** and **B** and the final complex **4**.

observations imply that there is an equilibrium between **A** and **B**. As the reaction proceeded, the multiplet pairs derived from **A** and **B** diminished without changing in ratio. There was also an accompanying decrease in the signal due to the acetato ligand in intermediate **B** and an increase in the signals due to **4**.

In 1982, Raymond et al. published the first definitive article on the displacement of the V=O bond of $VO(cat)_2^{2-}$ by catechol.[17] The displacement of the very stable V=O bond was highly dependent on the pH of the aqueous medium. A similar pH-dependent behavior was observed with $Ti(cat)_3^{2-}$.[14b,28a] Raymond et al. emphasized that the catecholato ligand has an exceptional chelating ability that can stabilize strong Lewis acid metal ions in a high oxidation state.[17] In early transition metal oxoporphyrins, the Ti=O bond of $Ti^{IV}O$(tpp) was displaced by catechol to give Ti^{IV}(cat)(tpp).[14b,18a,b] However, no other oxometalloporphyrin has been reported to show a metal−oxo cleavage by catechol. Vanadium(IV) and niobium(V) oxoporphyrins belonging to the vanadium group make especially stable metal−oxo bonds, as the oxo ligand of $V^{IV}O$(tpp) cannot be displaced by catechol. On the other hand, the oxo ligand can be cleaved and displaced by stoichiometric catechol in oxoniobiumporphyrins.

In niobiumoxoacetatoporphyrin, the Nb=O bond cleavage is initiated by the exchange of the acetato ligand with a catechol ligand, as shown in Scheme 1. The first catechol coordination is facilitated by the fast dissociation equilibrium of the axial acetato ligand of species **I**. Once catechol binds to the niobium(V) center with one hydroxyl group, the other hydroxyl group could form an intramolecular hydrogen bond to stabilize the structure (species **II**). The formation of species **II** is the most significant step in the cleavage of the metal−oxo bond. The niobiumporphyrins have a *cis*-configured hexacoordinate structure, whereas no vanadiumporphyrins are known to have this structure. The difference in the reactivity of the oxoniobiumporphyrins and the oxovanadiumporphyrins is due to the difference in their abilities to form an intermediate corresponding to species **II**. As mentioned above, the Ti=O bond is cleaved by the catechol. Although no definitive reaction mechanism has been proposed, an intermediate that has a structure similar to that of species **II** could be formed after the protonation of the Ti=O moiety. In support of this, a titaniumporphyrin of the *cis*-configured hexacoordinate structure has been reported.[18a] The reaction of the μ-oxo dimer with stoichiometric catechol also provided the final catecholato complex **3** or **4**, in which only intermediate **A** was observed. This observation led us to conclude that the reaction was initiated by the formation of species **II**, which was induced by an acid-base equilibrium between the μ-oxo ligand and a catechol. On the other hand, if the reaction is affected by the pH of the solvent, the displacement of TiO(tpp) must be initiated by protonation of the metal−oxo bond with catechol. Thus, the mechanism of displacement of the Nb=O bond is essentially different from that of TiO(tpp). By considering species **II**, **A** and **B** must be formed by the cleavage of the Nb=O bond, which is caused by the initially coordinated $Hcat^-$. If another catechol molecule assists in the cleavage by simple protonation of the oxo ligand to form a hydroxo ligand, the intermediates cannot be observed.

Therefore, we propose that an electron transfer (ET) mechanism cleaves the inert Nb=O bond. For comparison, we conducted some experiments with some other substrates. Two equivalents of 1,2-cyclohexanediol did not result in any reaction product with **1** or $\{Nb(tpp)\}_2O_3$ under the same conditions. This indicates the importance of the redox property of catechol as a potential reductant. In other words, the ET from catechol to the niobium(V) porphyrin complex is indispensable for Nb=O bond cleavage and ligand substitution. On the other hand, two equivalents of 2-methoxyphenol also did not show any reaction with **1**. This result clearly suggests that the intramolecular hydrogen bonding as proposed for species **II** also plays an important role in cleaving the Nb=O bond. This hydrogen bonding could reduce the bond strength of Nb=O so that it could be cleaved and accommodate ET from the catecholato to the niobium(V) center. Species **II** undergoes intramolecular one-electron and one-proton transfer from the monodentate catecholato ligand to the Nb=O moiety to form a putative and undetected Nb^{IV}(por)(OH)(semiquinone) complex (species **III**). In the case of the reaction of **1** with PhSH, we observed the formation of a niobium(IV) species by ESR spectroscopy.[32] Comparison of oxidation potentials of catechol and PhSH indicated that catechol is more easily oxidized than PhSH.[33] Thus, it is reasonable to expect that ET occurs from catechol to the niobium(V) center. These observations lend credence to our hypothesis that the intramolecular ET from catechol to the niobium(V) center is involved in the catechol coordination reaction.

The semiquinone ligand in species **III** can be reduced to form a catecholato ligand by reverse ET from the niobium(IV) center resulting in species **IV** followed by chelation of the bidentate catecholato ligand to the niobium center, or it can undergo radical coupling with the niobium(IV) center to form the observed intermediate Nb^V(por)(cat)(OH) (intermediate **A**). Que and co-workers used potassium *tert*-butoxide to deprotonate the hydroxyl group in the monodentate catecholato ligand to form a bidentate catecholato complex.[16] This implies a strong base is necessary for the deprotonation of monodentate catechol to enforce chelation. However, in our system, which does not contain any external base, the bidentate catechol formation mechanism should be different.

We have been unable to detect a coordinating OH group by ^{1}H-NMR spectroscopy. However, the intermediate **A** might react with another catechol molecule to form **4**, in which the

(32) Azuma, N.; Kurihara, M.; Matsuda, Y. Unpublished observation.
(33) Oxidation potentials of thiophenol and catechol in CH_2Cl_2 are 1.05 and 0.85 V vs $Ag/AgNO_3$, respectively.

Scheme 1

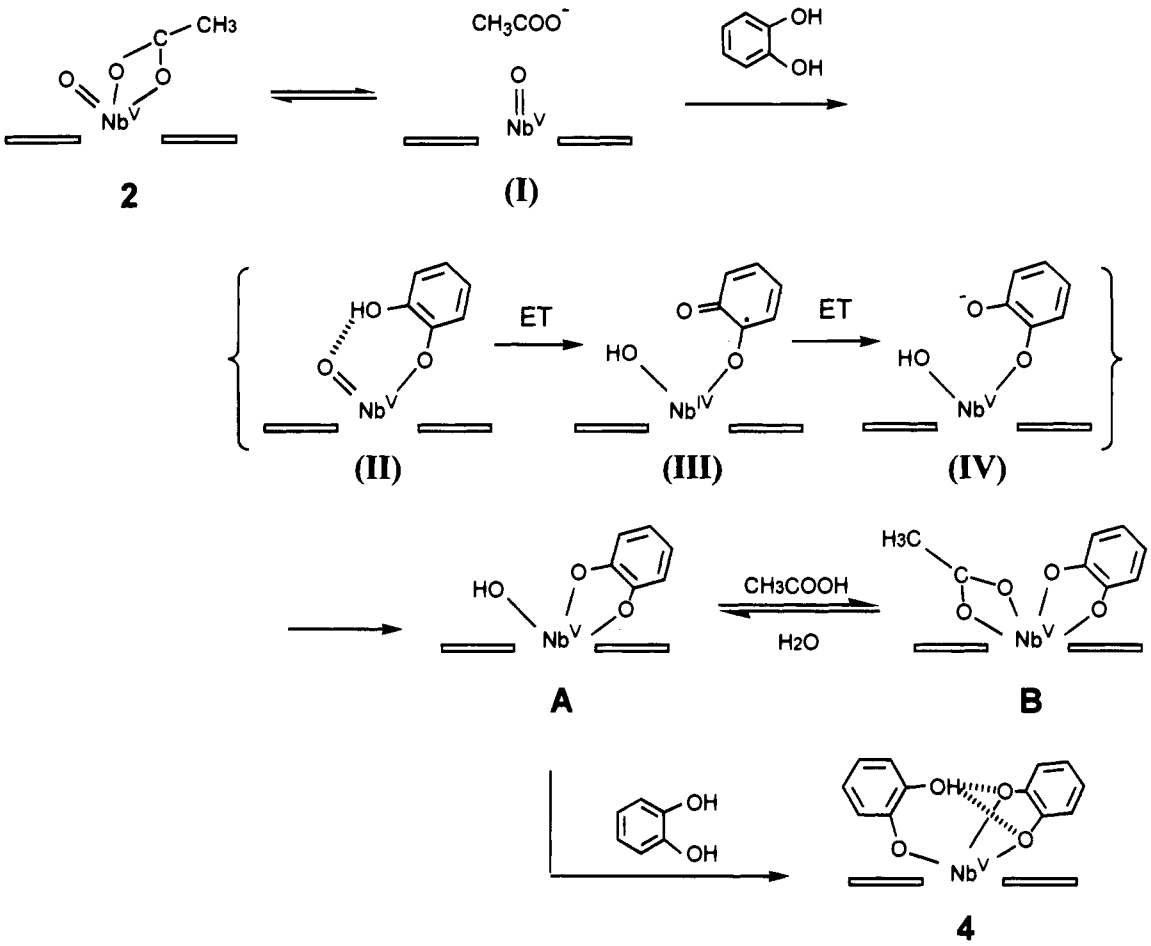

hydroxo ligand can act as a proton acceptor. As the coordination of the second catechol proceeds, intermediate **A** is supplied by the hydrolysis of intermediate **B** via an equilibrium shift. In the final step of coordination of the second catechol, the OH group of **A** can act as a base to deprotonate catechol. Catecholate can then bind to the niobium(V) ion followed by the formation of an intramolecular hydrogen bond between the two catechol molecules. The hydrogen bond could be another driving force for the binding of the second catecholato ligand and a stabilizing factor of **4**.

Summary

This study characterizes niobium(V) porphyrin complexes, including catecholato complexes, and presents mechanistic insights into catechol coordination concomitant with the Nb=O bond cleavage. X-ray crystallography of one of the catecholato complexes, Nb(tpp)(cat)(Hcat) (**3**), revealed a unique structure containing two distinct catecholato ligands on the same side of tpp, one bidentate and one monodentate, and joined by an intramolecular hydrogen bond. On the other hand, the metal-bound catechols described here do not show any semiquinone character, unlike the catechol-semiquinone tautomerization complexes reported by Pierpont and co-workers,[13] and do not show intradiol cleavage in the presence of dioxygen, as reported by Que and co-workers.[34] The difference may be due to the intramolecular hydrogen bonding, which can weaken the ability of catechol and the metal center to undergo intramolecular ET, and thus prevent it from having a semiquinone character. The redox chemistry of the photochemical behavior of this new category of catecholato complex is currently being investigated in our laboratory.

The reaction mechanism of catechol coordination has been established by ^{1}H-NMR spectroscopy at −30 °C to involve two different intermediates having bidentate catechols. One intermediate possesses an axial acetato ligand and the other presumably has a hydroxo ligand that can act as a base to deprotonate the second catechol molecule. Although direct evidence is lacking, we favor a reaction mechanism involving intramolecular electron and proton transfer from the catechol to a Nb^V(por)(O) complex for the cleavage of the Nb=O bond. To our knowledge, this is a novel pathway for the activation of an inert Nb=O bond.

Acknowledgment. We are grateful to Ms. Mie Tomonou for her helpful assistance in obtaining NMR spectra. We are also grateful to Prof. Masanobu Hidai (the University of Tokyo) for making X-ray crystallography possible. This work was supported by Grants-in-Aid for Scientific Research (Nos. 04453047 and 05209223) from the Ministry of Education, Science, and Culture.

Supporting Information Available: Text detailing the structure determination, tables of atomic coordinates, crystallographic data, thermal parameters, bond lengths and angles, torsion angles, and ORTEP drawings with full numbering scheme, ^{1}H-NMR spectrum of the complex **4**, two dimensional *J*-resolved spectrum of **4**, and ^{1}H−^{1}H COSY spectrum of the catechol region of **4** and **5** (39 pages). Ordering information is given on any current masthead page.

IC941214I

(34) (a) Que, L., Jr.; Kolanczyk, R. C.; White, L. S. *J. Am. Chem. Soc.* **1987**, *109*, 5373. (b) Jang, Ho. G.; Cox, D. D.; Que, L., Jr. *J. Am. Chem. Soc.* **1991**, *113*, 9200.